Arabinoxylan structure affects the reinforcement of films by microfibrillated cellulose

Kirsi S. Mikkonen · Leena Pitkänen · Ville Liljeström ·
Elina Mabasa Bergström · Ritva Serimaa ·
Lennart Salmén · Maija Tenkanen

Abstract The chemical structure of rye arabinoxylan (rAX) was systematically modified, exploiting selective enzymes to mimic different naturally occurring xylans, i.e., its degree of substitution (DS) was decreased using α-L-arabinofuranosidase, and a controlled decrease in the degree of polymerization (DP) was performed using endo-1,4-β-D-xylanase. The arabinose to xylose ratio was decreased from 0.45 to 0.27 and the weight-average molar mass was decreased from 184,000 to 49,000 g/mol. The resulting samples were used to prepare films, as such, and with 15% (wt. $-$ %) softwood-derived microfibrillated cellulose (MFC) to obtain novel plant-derived biocomposite materials. The enzymatic tailoring of rAX increased the crystallinity of films, evidenced by X-ray diffraction studies, and the addition of MFC to the debranched, low DS rAX induced the formation of ordered structures visible with polarizing optical microscopy. MFC decreased the moisture uptake of films and increased the relative humidity of softening of the films, detected with moisture scanning dynamic mechanical analysis. For the first time, the chemical structure of xylan was proven to significantly affect the reinforcement potential of nano-sized cellulose, as the tensile strength of films from high DP rAXs, but not that of low DP rAXs, clearly increased with the addition of MFC. At the same time, MFC only increased the Young's modulus of films from rAX with high arabinose content, regardless of DP.

Keywords Arabinosidase · Arabinoxylan · Composites · Films · Microfibrillated cellulose · Xylanase

Introduction

During recent decades, polysaccharides have been widely studied as raw materials for biodegradable and edible films (Nisperos-Carriedo 1994; Guilbert et al. 1996). Polysaccharides are more sustainable than conventional plastics, because they are isolated from renewable raw materials and their production requires less non-renewable energy and yields fewer greenhouse gas emissions than the production of synthetic materials (Shen and Patel 2008). Polysaccharide-based films are generally good barriers against grease and oxygen gas, but their properties are usually

K. S. Mikkonen (✉) · L. Pitkänen · M. Tenkanen
Department of Food and Environmental Sciences,
University of Helsinki, P.O. Box 27,
00014 Helsinki, Finland
e-mail: kirsi.s.mikkonen@helsinki.fi

V. Liljeström · R. Serimaa
Department of Physics, University of Helsinki,
P.O. Box 64, 00014 Helsinki, Finland

E. Mabasa Bergström · L. Salmén
INNVENTIA AB, Fibre & Material Science,
Box 5604, 114 86 Stockholm, Sweden

sensitive to changes in ambient relative humidity (RH), and the barrier properties against water vapor are poor at high RH (Nisperos-Carriedo 1994; Gröndahl et al. 2004; Mikkonen et al. 2009; Mikkonen et al. 2010a, b).

Hemicelluloses are the most abundant plant polysaccharides apart from cellulose. The most abundant hemicelluloses are xylans, which constitute 25–35% of the dry biomass of woody tissues of dicots and lignified tissues of monocots (Ebringerová and Heinze 2000). Many agricultural crops, as well as forest and pulping side streams, are potential sources for xylans. Up to 40% of some tissues in cereal grains, such as oat spelts, consist of xylans (Hettrich et al. 2006). Cereal arabinoxylans consist of $(1 \rightarrow 4)$-linked β-D-xylopyranosyl backbones, to which groups of α-L-arabinofuranosyl units are connected by $(1 \rightarrow 3)$- and/or $(1 \rightarrow 2)$-glycosidic linkages at irregular intervals (Izydorczyk and Biliaderis 1995). In rye endosperm arabinoxylan (rAX), the backbone units are both mono- and di-substituted by α-L-arabinofuranosyl units with a ratio of mono- and di-substituted xylopyranosyl residues of 2:1 and an average arabinose to xylose (Ara/Xyl) ratio of 0.50 (Pitkänen et al. 2009). Other naturally occurring xylans differ from rAX in their branching and molar mass; e.g., oat spelts and softwoods contain arabinoglucuronoxylans, which have $(1 \rightarrow 3)$-linked α-L-arabinofuranosyl units and $(1 \rightarrow 2)$-linked 4-O-methyl-α-D-glucopyranosyluronic acid (MeGlcA) units with an Ara/MeGlcA/Xyl ratio of 1.2:0.4:10 and 1:2:10, respectively (Ramírez et al. 2008; Sjöström 1993). The molar mass of cereal endosperm arabinoxylans (250,000–300,000 g/mol) (Pitkänen et al. 2009) is clearly higher than that of oat spelt arabinoxylan (32,000 g/mol) (Ramírez et al. 2008), wheat straw arabinoxylan (25,000–30,000 g/mol) (Sun et al. 2000), and softwood arabinoglucuronoxylan (15,000 g/mol) (Sjöström 1993). The chemical structure, especially the branching, affects the solubility properties, and the less substituted arabino(glucurono)xylans are generally less water soluble than highly substituted xylans (Zhang et al. 2011).

Xylans are a remarkable natural resource, but there are currently no industrial processes utilizing isolated xylans, although patents and studies exist, for example, on the use of xylans as raw materials for biodegradable films and as paper chemicals (Gatenholm et al. 2008; Gröndahl et al. 2008; Köhnke et al. 2008; Ramírez et al. 2008). To further develop the use of xylans as

packaging films, it is essential to study their structure–function properties in detail. The relatively high molar mass and highly branched chemical structure of rAX offer possibilities for modifications. Controlled acid hydrolysis of rAX resulted in a decreased degree of arabinofuranosyl substitution (DS) but, concomitantly, the degree of polymerization (DP) was also decreased (Sternemalm et al. 2008). Films from acid hydrolyzed rAX showed decreased moisture uptake at 98% RH and softened at higher RH than films from native rAX (Sternemalm et al. 2008). Enzymes offer more controlled ways of making biopolymer modifications due to their high specificity, and are thus invaluable tools in structure–function studies of natural polymers. Selective enzymatic debranching of rAX has lately been shown to decrease the oxygen permeability of films, and the tensile properties reached a maximum when the DS was slightly decreased (Höije et al. 2008). In our preceding work, films from enzymatically debranched rAX showed higher crystallinity and brittleness, and lower softening and water sorption in comparison to films from native rAX (Stevanic et al. 2011).

The mechanical performance of films can be improved using nanosized cellulose as reinforcement. Microfibrillated cellulose (MFC) is produced using high-pressure homogenization of wood pulp fibers in water and is mainly composed of liberated semicrystalline microfibrils with a width of 5–15 nm and a length of up to 1 µm (Wågberg et al. 2008). MFC as such can also be used to form films with high tensile strength and transparency (Sehaqui et al. 2010). In our previous study, the addition of MFC in spruce galactoglucomannan films remarkably increased their tensile strength and storage modulus (Mikkonen et al. 2011). Reinforcement of rAX with bacterial cellulose resulted in stronger and stiffer films (Stevanic et al. 2011). Cellulose nanowhiskers have also been used to increase the tensile strength of arabinoxylan films (Saxena et al. 2009). Recently, bamboo xylan films showed high reinforcement by cellulose nanofibers prepared from bleached sisal pulp (Peng et al. 2011). The use of wood-derived MFC, which is a more feasible nano-sized cellulose for industrial use than bacterial cellulose or cellulose nanowhiskers, has not previously been studied as a reinforcement of cereal arabinoxylan films. The aim of the present study was to thoroughly examine the effects of the structure of arabinoxylan and the addition of MFC on the

properties of self-standing films. Our innovative approach was to use enzymes as specific tools to tailor the DS and DP of rAX to mimic naturally-occurring arabinoxylans in different cereal and softwood sources.

Experimental section

Materials

High molar mass rye endosperm arabinoxylan (rAX) (lot 20601a) was purchased from Megazyme (Wicklow, Ireland). A mono-component endo-1,4-β-D-xylanase preparation, Shearzyme (49,075 nkat/ml) and endoxylanase-free α-arabinofuranosidase (9,245 nkat/ml) were from Novozymes (Bagsvaerd, Denmark). The Shearzyme cleaves the linkage between consecutive xylopyranosyl residues in the backbone of rAX, and the α-arabinofuranosidase efficiently liberates the α-L-arabinofuranosyl residues from the mono-substituted β-D-xylopyranosyl units (Höije et al. 2008). Anhydrous methanol (Sigma-Aldrich, Germany), acetyl chloride (Sigma-Aldrich), pyridine (Merck, Germany), TMSCl (chlorotrimethylsilane; Fluka, Switzerland), and BSTFA (bis-(trimethylsilyl)trifluoroacidamide; Merck) were used for acid methanolysis and silylation of the samples and L(+)-arabinose, D(+)-xylose, and D(+)-glucose (Merck) were used as monosaccharide standards in gas chromatography (GC). HPLC grade dimethyl sulfoxide (DMSO) was from Lab-Scan (Dublin, Ireland) and lithium bromide (LiBr) was from Sigma-Aldrich. MFC, which was generously provided by Mikael Ankerfors (Innventia, Sweden), was prepared from softwood sulphite pulp (Domsjö Dissolving Plus, Domsjö Mills, Sweden) according to a method previously developed (Pääkkö et al. 2007). The pulp suspension was first subjected to a pretreatment step involving mechanical beating and enzymatic treatment. The pretreated pulp suspension was then mechanically disintegrated by a homogenization process using a Microfluidizer M-110EH (Microfluidics Inc., Newton, MA, USA). A MFC-water suspension with a concentration of 0.22% (w/v) was obtained.

Enzymatic modification of rye arabinoxylan

Stepwise enzymatic modifications were carried out by treating rAX first with Shearzyme and then with α-arabinofuranosidase. Control samples were treated similarly but without the addition of enzymes. The rAX was dissolved in 25 mM sodium acetate buffer, pH 5.0, at 1% (w/v), heating it at 80 °C under magnetic stirring for 10 min. The solution was stirred overnight at room temperature. Decreasing the degree of polymerization (DP) of rAX was carried out by a treatment with Shearzyme using an endoxylanase dosage of 25 nkat/g of rAX. To select this dosage, preliminary experiments were carried out on a small scale, aiming to find an endoxylanase dosage that decreases the weight-average molar mass of rAX to approximately 50,000 g/mol. The rAX solution containing Shearzyme (rAX-L) and the control solution without enzyme (rAX-H) were incubated for 2 h at 40 °C with magnetic stirring. After incubation, the enzyme action was terminated by keeping the solutions in a boiling water bath for 15 min. Partial debranching of rAX was carried out by adding a moderate dosage of α-arabinofuranosidase (3,000 nkat/g) to the cooled solutions (rDAX-H and rDAX-L) and incubating them and the control solutions (rAX-H and rAX-L) for 66 h at 40 °C with magnetic stirring. The enzymatic treatment was terminated similarly as after the Shearzyme treatment. The arabinoxylan solutions were dialyzed for 48 h (MWCO 12–14,000 Da) against water to remove buffer ions and released short xylan fragments and arabinose. Samples of 2.5 mL were frozen and lyophilized for the estimation of the dry matter content of solutions/suspensions and for the determination of the molar mass of rAXs. The rest of the samples were kept as water solutions/suspensions prior to their use for film preparation, as the resolubilization of dried debranched rAX samples in water is difficult.

Structural analysis of rye arabinoxylan

The Ara:Xyl ratios of modified rAXs and the control sample were studied using GC after acid methanolysis following the method of Sundberg et al. (1996). The monosaccharide standards used were D-xylose, L-arabinose, and D-glucose. Quantification was performed, using six concentration levels of each sugar. The GC instrument used was an Agilent 6890 N GC system (Agilent Technologies, Foster City, CA, USA) with a flame ionization detector (FID). The system was equipped with an Agilent 7683 series injector and autosampler using Agilent ChemStation 06 software for instrument control and data handling. The column

used was a DB-1 (30 m, 0.25-mm i.d., 0.25-µm film thickness) from Agilent Technologies. The analysis of the silylated monosaccharides was performed, using a gradient system with a total run time of 41.25 min. The initial temperature of 150 °C was held for 3 min and three linear gradients were followed: (1) 2 °C/min from 150 to 186 °C, (2) 1 °C/min from 186 to 200 °C, and (3) 20 °C/min from 200 to 325 °C.

The M_w of the rAX samples was determined by high performance size exclusion chromatography (HPSEC) in DMSO eluent containing 0.01 M LiBr. The equipment and the method of HPSEC analysis used was according to Pitkänen et al. (2009).

Preparation of films

Films were prepared from enzymatically treated rAXs (rDAX-H, rAX-L, and rDAX-L) and the control sample (rAX-H) with and without the addition of MFC. The rAX:MFC weight ratio used was 85:15. No external plasticizer was added. In addition, a film was also prepared from plain MFC to be used as a reference sample in X-ray diffraction and water sorption studies. Sample codes are shown in Table 1. The rAX solutions, rAX-MFC mixtures, and MFC suspension were heated under magnetic stirring at 60 °C and homogenized using an Ultra-Turrax (Ika-Werke, Staufen, Germany) at 9,500 rpm for 10 min. The MFC suspension was concentrated by magnetic stirring in vacuum from 0.22% (w/v) to approximately 0.5%. The suspensions were cast into Teflon-coated Petri dishes (diameter 9.4 cm), and dried at 23 °C and 50% RH. The thickness of the films was approximately 30–40 µm.

Microscopy

Optical imaging of the films was done with a Zeiss AxioScope A1 polarizing optical microscope (OM) (Carl Zeiss Inc., Oberkochen, Germany) equipped with an AxioCam ICc3 camera, using transmitted light.

X-ray diffraction

Wide-angle X-ray diffraction measurements were carried out to characterize the crystallinity of xylan in the films. The diffraction patterns of the rAX films and a plain MFC film were measured. The measurements were done in the perpendicular transmission geometry using a sealed X-ray tube (point focus, PANalytical, Almelo, The Netherlands), and Cu K_α radiation (wavelength 1.54 Å). The beam was monochromated using a collimating Montel multilayer monochromator (Incoatec, Geesthacht, Germany) and the diffraction pattern was measured with a MAR345 image plate detector (Rayonix, Evanston, IL, USA).

Two-dimensional diffraction patterns were spherically averaged to one-dimensional diffraction intensity profiles and corrections in the intensity profiles were made to take the attenuation in the sample and the differences in diffracted ray paths due to the use of a plate detector into account. Calibration of the angular range was made using the known diffraction maxima of silver behenate, silicon and aluminum standard samples. The broadening of the diffraction maxima on the whole angular range due to the instrument was estimated to be $0.2 \pm 0.1°$. This estimate was done using the silver behenate peaks at low scattering angles and an aluminum diffraction

Table 1 Film codes

Code	Description
rAX-H	Film with 100% high DP rye arabinoxylan (high DS)
rAX-H:MFC	Film with 85% high DP rye arabinoxylan + 15% microfibrillated cellulose
rDAX-H	Film with 100% high DP debranched rye arabinoxylan (low DS)
rDAX-H:MFC	Film with 85% high DP debranched rye arabinoxylan + 15% microfibrillated cellulose
rAX-L	Film with 100% low DP rye arabinoxylan (high DS)
rAX-L:MFC	Film with 85% low DP rye arabinoxylan + 15% microfibrillated cellulose
rDAX-L	Film with 100% low DP debranched rye arabinoxylan (low DS)
rDAX-L:MFC	Film with 85% low DP debranched rye arabinoxylan + 15% microfibrillated cellulose
MFC	Film with 100% microfibrillated cellulose

peak at high scattering angles. All of the diffraction measurements were carried out under ambient conditions, e.g., room temperature and low humidity. All film samples were stacked multifold during the measurement to gain a sample thickness of 0.31 ± 0.03 mm on average. Hence the statistical accuracy of the diffraction intensity was improved.

To determine the crystallinity index, a linear combination of the diffraction patterns of crystalline and amorphous arabinoxylan and MFC were fitted to each experimental intensity curve. In the fitting procedure the diffraction pattern of crystalline arabinoxylan was computed on the basis of the known crystal structure of xylan dihydrate (Nieduszynski and Marchessault 1972) and the widths and intensities of the diffraction peaks; in addition, the lattice constants a and c were used as fitting parameters. PowderCell 2.3 software (Institute for Molecules and Materials, Radboud University Nijmegen, Nijmegen, The Netherlands) was used to obtain the relevant peaks included in the fit. The non-crystalline background was measured from rAX-H film that was assumed to have a crystallinity of 0%. For this reason the crystallinity values are not absolute values, but are relative to this non-crystalline background.

The crystallinity, ϕ, was evaluated according to Eq. (1):

$$f = 1 - \left(\sum I_{amorph} / \sum I_{measured} \right), \qquad (1)$$

where I_{amorph} denotes the non-crystalline scattering part of the intensity profile and $I_{measured}$ denotes the total intensity profile. From diffraction patterns of samples containing MFC, the MFC contribution to $I_{measured}$ was deducted; thus in all cases the crystallinity represents the crystallinity of arabinoxylan. The widths of the crystallites were determined from the most well resolved diffraction peaks, namely the 100 and 011 peaks (Guinier 1994).

Light transmittance

The light transmittances of the films were scanned at wavelengths from 190 to 800 nm using a Shimadzu UV-2501 PC spectrophotometer (Kyoto, Japan) equipped with an integrating sphere detector. The measurement was done in triplicate and the average of the three spectra was calculated. In addition, the haze of the films was determined in duplicate at a wavelength of 550 nm as described in the ASTM Standard Test Method for Haze and Light Transmittance of Transparent Plastics (ASTM 2007).

Water sorption

A DVS Intrinsic sorption microbalance (Surface Measurement Systems, Alperton, Middlesex, UK) was used in order to collect water sorption isotherms. The experiments were carried out in duplicate at 25 °C and RH values from 0 to 90%. The sample was hydrated stepwise in 10% RH steps by equilibrating the sample weight at each step. The moisture uptake was calculated according to Eq. 2:

$$Moisture\,uptake = 100 \frac{W_{moist} - W_{dry}}{W_{dry}}, \qquad (2)$$

where W_{moist} is the sample weight equilibrated at the chosen relative humidity and W_{dry} is the weight of the dry sample.

Mechanical properties

Dynamic mechanical analysis (DMA) was carried out using a Perkin-Elmer DMA 7e (PerkinElmer Corp., Norwalk, CT, USA). The film specimens with dimensions of 2 mm × 20 mm × 30 μm (width × length × thickness) were first conditioned at 0% RH and then scanned in a range of 1–90% RH at a speed of 1% RH/5 min at a temperature of 30 °C. The desired relative humidities were achieved by mixing dry air and water-saturated air using a Wetsys humidity generator (Setaram Instrumentation, Caluire, France). The static load was adjusted to be equal to 120% of the dynamic load, the amplitude was set to be constant at 5 μm, and a frequency of 1 Hz was applied. The storage modulus (E') was recorded using Pyris DMA 28 software (PerkinElmer Corp., Norwalk, CT, USA).

The tensile strength, elongation at break, and Young's modulus of the films were determined at 23 °C and 50% RH (climate room) using an Instron 4465 universal testing machine with a load cell of 100 N. The initial grip distance was 50 mm and the rate of grip separation was 5 mm/min. Nine to 12 replicate specimens from each film type were measured except from the rDAX-L:MFC film, which was so brittle that only three replicate specimens could be measured. The specimens were 5 mm wide and

approximately 70 mm long. The thickness of the specimens was measured with a micrometer (Lorentzen & Wettre, Sweden, precision 1 μm) at three points and an average was calculated.

Statistical analyses

One-way analysis of variance (ANOVA) was used to test the differences in the tensile properties of the films. Tukey's test was used for pairwise comparison of the means. In addition, the effects of the DS, DP, and MFC as well as their interaction effects on the tensile strength, elongation at break, and Young's modulus were evaluated using contrasts, which is a flexible way to highlight differences in the data (Mikkonen et al. 2007). To obtain the contrast values, the results of the different levels of each factor were multiplied with coefficients, shown in Table 2, and then summed up. The coefficients were selected so that the absolute sum of coefficients with the same sign is one and the sum of all coefficients is zero. Thus the sign of the obtained contrast depends on the selection of the coefficients and if the absolute value of the obtained contrast is large, the results differ from each other. Differences were considered statistically significant when p was ≤ 0.05. SPSS 15.0.1 (SPSS Inc., Chicago, IL) was used for the analyses.

Results and discussion

Chemical composition

The α-arabinofuranosidase used has specificity only towards the α-L-arabinofuranosyl units linked to the mono-substituted xylopyranosyl residues (Höije et al.

2008). According to the GC analysis, 40% of the total α-L-arabinofuranosyl units were removed from rAX-H and rAX-L, and the resulting Ara:Xyl ratios of the debranched rye arabinoxylans were 0.27 for rDAX-H and 0.26 for rDAX-L (Table 3). As two-thirds of the arabinofuranosyl units of native rAX are attached to mono-substituted xylopyranosyl units and one-third on di-substituted units (Pitkänen et al. 2009), 12 and 11% of xylopyranosyl units of rDAX-H and rDAX-L, respectively, were mono-substituted and 7.5% were di-substituted. This indicates that the enzymatic debranching was successful, although not all arabinofuranosyl residues accessible to the enzyme used were released due to the moderate enzyme dosage applied, as the target was to prepare rAX samples with Ara:Xyl ratios of about 0.25, in contrast to our preceding work, which aimed at maximal removal of arabinofuranosyl residues from the mono-substituted xylopyranosyl units of rAX (Stevanic et al. 2011).

The molar mass of rAXs was studied using HPSEC in DMSO containing 0.01 M LiBr, which is known to be a good solvent for arabinoxylans (Pitkänen et al. 2009). The molar mass distributions obtained are presented in Fig. 1, and weight-average molar masses and dispersity indexes are shown in Table 3. The applied Shearzyme treatment reduced the weight-average molar mass of rAX from 184,000 to 49,000 g/mol. However, the treatment clearly increased the poly-dispersity of the samples. Although the chain length of the sample was mostly reduced, some intact molecules existed in the Shearzyme-hydrolyzed sample. This might be due to the inability of the endoxylanase to act on the most highly substituted xylan chains, as water-extracted arabinoxylan samples from rye flour are heterogeneous and may well contain structurally diverging populations of arabinoxylans

Table 2 Contrast coefficients used to compare levels of factors with respect to averages of tensile strength, elongation at break, and Young's modulus

Film	Factors			Interactions		
	DS	DP	MFC	DS/DP	MFC/DS	MFC/DP
rAX-H	−0.25	−0.25	−0.25	−0.25	−0.25	−0.25
rAX-H:MFC	−0.25	−0.25	0.25	−0.25	0.25	0.25
rDAX-H	0.25	−0.25	−0.25	0.25	0.25	−0.25
rDAX-H:MFC	0.25	−0.25	0.25	0.25	−0.25	0.25
rAX-L	−0.25	0.25	−0.25	0.25	−0.25	0.25
rAX-L:MFC	−0.25	0.25	0.25	0.25	0.25	−0.25
rDAX-L	0.25	0.25	−0.25	−0.25	0.25	0.25
rDAX-L:MFC	0.25	0.25	0.25	−0.25	−0.25	−0.25

Table 3 Arabinose to xylose ratios and weight-average molar masses of modified rAX samples

	Ara:Xyl	Molar mass (Da)	Dispersity index (M_w/M_n)
rAX-H	0.45	184,000	1.2
rDAX-H	0.27	152,000	1.1
rAX-L	0.43	49,000	5.2
rDAX-L	0.26	59,000	2.3
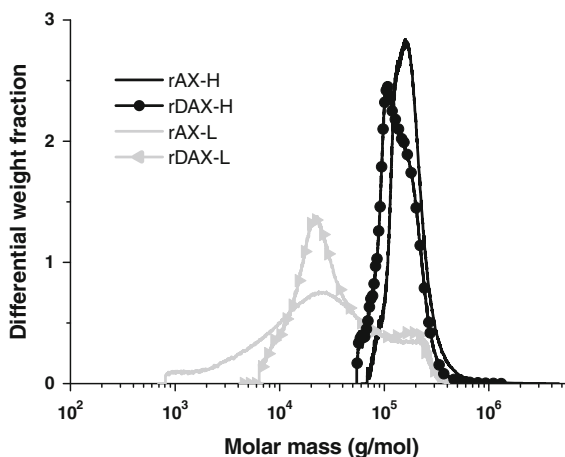
Fig. 1 Molar mass distributions obtained with HPSEC in DMSO with 0.01 M LiBr

(Bengtsson et al. 1992). The α-arabinofuranosidase treatment shifted the molar mass distribution of rAX-H slightly to the direction of lower molar mass, as expected, but the Shearzyme intact part of the rAX-L sample, which might be highly substituted, seemed to also be resistant to the α-arabinofuranosidase action. The rAX-L sample contained lower molar-mass molecules (in a mass range of 800–6,000 g/mol) that cannot be observed in the molar mass distribution of the rDAX-L sample. The explanation could lie in the disappearance of short rDAX-L chains during dialysis due to a decrease in the molecular size as a result of arabinose removal. The rAX-L and rDAX-L samples were used for film preparation without further fractionation, although they were highly poly-dispersed.

Morphology

All rAX samples with or without MFC, even those with low DS and DP (rDAX-L), formed cohesive, self-standing films without an external plasticizer. However, the film prepared from rDAX-L with MFC was very brittle. When viewed with polarizing OM, there were no visible structures in any of the plain rAX films, but the composite films with MFC showed bright polarizing fibers and textures indicating ordered structures (Fig. 2). Films from rAX-H:MFC and rAX-L:MFC contained relatively large fiber structures with lengths of up to 100 micrometers and widths of several micrometers (Fig. 2a, c), similar to those seen by polarizing OM in spruce galactoglucomannan-MFC composite films and considered to be cellulose fiber residues (Mikkonen et al. 2011). The nano-sized fibrils are not visible at the magnifications used. In contrast, composite films from low DS rDAXs (rDAX-H:MFC and rDAX-L:MFC) had polarizing textures seemingly formed from MFC and rDAX together, indicating interactions between these two components (Fig. 2b, d).

From the X-ray diffraction pattern of partly crystalline rDAX films, the crystal structure of arabinoxylan was recognized to be hexagonal. The X-ray diffraction measurements revealed remarkable differences between the crystallinity and the average crystallite sizes of xylan in the samples. Films from high DS rAXs showed only minimal, if any, crystalline character. A barely noticeable distinction from the non-crystalline background could be seen in the diffraction patterns of the rAX-L and rAX-L:MFC films. On the other hand, all films from low DS rDAXs, with or without MFC reinforcement, clearly showed a crystalline character (Fig. 3). The xylan crystallinity and the average crystallite widths, determined from reflections 100 and 011, were significantly higher for rDAX-L and rDAX-L:MFC films than for rDAX-H and rDAX-H:MFC films (Table 4). This could result from the higher mobility and capacity to form ordered structures of low DP rDAX compared to high DP rDAX. The crystallite widths of rDAX-H:MFC and rDAX-L:MFC composite films did not significantly differ from those of plain rDAX-H and rDAX-L films. The lattice parameters a and c were slightly higher for the MFC-reinforced films from low DS rDAXs than for the corresponding films without MFC. The diffraction pattern of the plain MFC film was found to fit into the measured diffraction patterns from MFC-reinforced rAX films, which confirms that the microstructure of MFC was unchanged when used as reinforcement.

The crystallinities of xylan in rDAX-H and rDAX-L films (11 and 17%, respectively) were lower than those found earlier for rDAX films (20%) (Stevanic et al. 2011). In this preceding work, a more efficient enzymatic debranching was applied, resulting in an
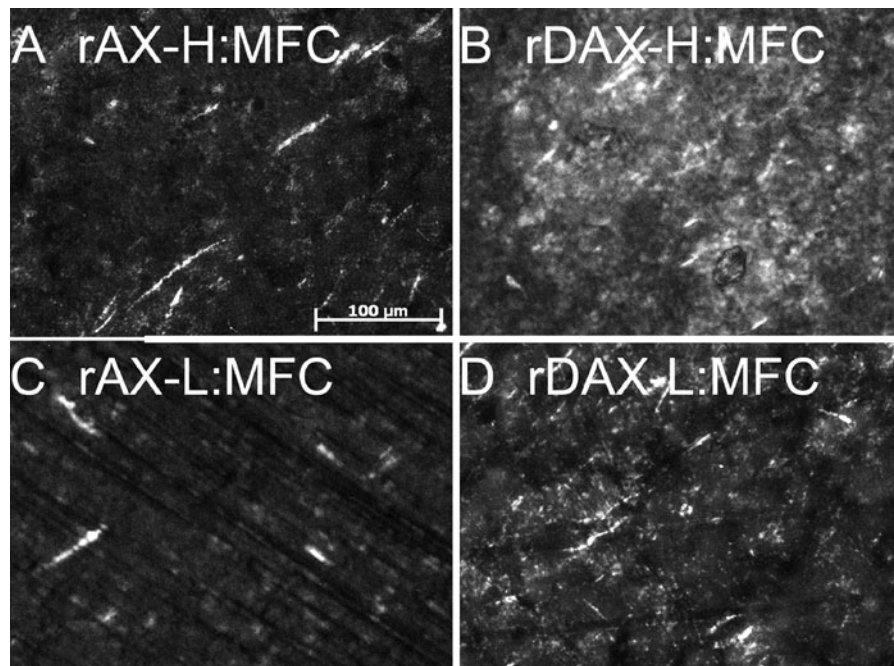
Fig. 2 Polarizing optical microscopic images of films from **a** rAX-H:MFC, **b** rDAX-H:MFC, **c** rAX-L:MFC, and **d** rDAX-L:MFC. The *scale bar* in A is 100 μm and all images are at the same magnification

Ara:Xyl ratio of 0.16, which may explain the higher crystallinity of those films. Polyol-plasticized oat spelt arabinoxylan (osAX) films also showed a crystallinity between 20 and 26% (Mikkonen et al. 2009). The DS and DP of osAX are low, which both may enhance the crystallization, in addition to the plasticizer. The presence of MFC did not affect the crystallinity of xylan in rAX films, analogous to what was reported for MFC-reinforced galactoglucomannan films (Mikkonen et al. 2011) and rAX-bacterial cellulose composite films (Stevanic et al. 2011).

Light transmittance

All films had high light transmittance in the visible region of the spectrum, indicating that the films were transparent (Table 5). The differences in the light transmittance of films were small, but because of low standard deviations, some trends can be seen. The light transmittance of films at the 550 nm wavelength slightly decreased when MFC was added. In addition, the light transmittance of films from high DS rAXs was higher than that of films from low DS rDAXs. The

rAX-H film had the highest light transmittance and the rDAX-H:MFC film had the lowest.

Haze is the scattering of light by a specimen responsible for the reduction in contrast of objects viewed through it (ASTM 2007). The films differed greatly in haze (Table 5). The addition of MFC clearly increased the haze of films, especially that of films from high DP rAXs. The highest haze was measured for the rDAX-H:MFC film. This indicates, similarly to the polarizing OM images of that film, that rDAX-H and MFC interacted and formed structures detectable with microscopy and spectrophotometer. The haze of films from low DP rAXs was lower than that of films from high DP rAXs.

Water sorption

The water sorption isotherms of all films displayed a sigmoidal shape generally reported for hydrophilic materials (Fig. 4). As expected, plain MFC absorbed less water than the rAX-based films. In addition, the presence of MFC slightly decreased the moisture uptake of the rAX-MFC composite films.
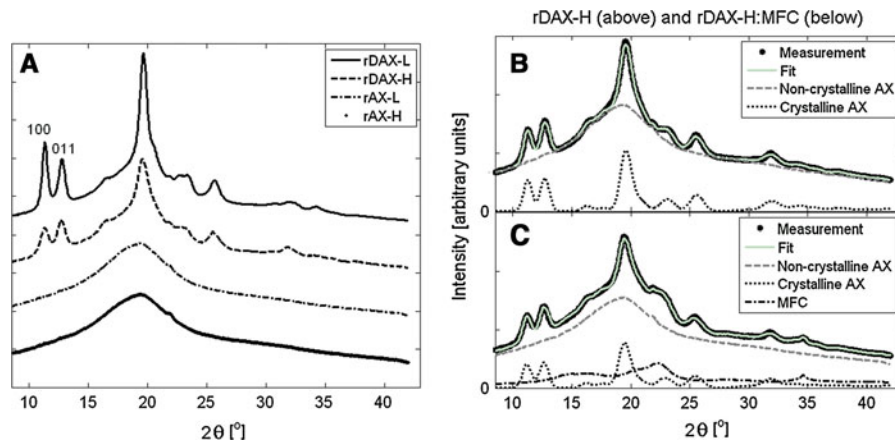
Fig. 3 a The diffraction patterns of films not containing MFC and diffraction patterns of b rDAX-H and c rDAX-H:MFC films plotted together with the non-crystalline background scattering, the model for the crystalline scattering, and the contribution of scattering from MFC to the intensity profile. The profile fitted to the data points is a linear combination of the experimental diffraction pattern of non-crystalline arabinoxylan, the crystalline model, and the experimental pattern of MFC. The intensity profiles are plotted as a function of scattering angle 2θ (°)

Table 4 Crystallinity index, crystallite size, and lattice constants of xylan in the films determined by wide angle X-ray scattering

Sample	ϕ (%)	Crystallite size (100) (Å)	Crystallite size (011) (Å)	Lattice constants a and b (Å)	Lattice constant c (Å)
rAX-H	0	–[a]	–	–	–
rAX-H:MFC	0.5 ± 2	–	–	–	–
rDAX-H	11 ± 2	99 ± 7	101 ± 7	9.06 ± 0.02	15.02 ± 0.10
rDAX-H:MFC	11 ± 2	96 ± 7	91 ± 6	9.12 ± 0.02	15.06 ± 0.10
rAX-L	1.6 ± 2	–	–	–	–
rAX-L:MFC	1.7 ± 2	–	–	–	–
rDAX-L	17 ± 3	158 ± 21	144 ± 17	9.03 ± 0.02	15.04 ± 0.10
rDAX-L:MFC	21 ± 3	142 ± 16	124 ± 12	9.07 ± 0.02	15.13 ± 10

[a] Not detected

Table 5 Light transmittance and haze of films at 550 nm ± standard deviation

| Film	Transmittance (550 nm) (%)	Haze (550 nm) (%)
rAX-H	89.4 ± 0.3	11.0 ± 0.2
rAX-H:MFC	87.1 ± 0.5	34.5 ± 0
rDAX-H	88.3 ± 0.6	9.2 ± 0.4
rDAX-H:MFC	84.9 ± 0.9	63.1 ± 0.1
rAX-L	88.8 ± 0.1	8.35 ± 2.3
rAX-L:MFC	88.3 ± 0.2	22.3 ± 0.1
rDAX-L	87.8 ± 0.3	6.8 ± 0.1
rDAX-L:MFC	86.1 ± 0.4	25.0 ± 0.8

Previously, the moisture uptake of arabinoxylan films at RH below 80% was considered to be governed by water bound by the arabinoxylan sorption sites and, above that, increased due to swelling by water (Zhang et al. 2011). Also in the present study, the water content difference of films was highest between 80 and 90% RH. At 60–80% RH, the moisture uptake of films from low DS rDAXs was slightly higher than that of films from high DS rAXs but, at the highest RH studied (90%), there were no considerable differences. In comparison, Höije et al. (2008) found that decrease in the DS of rAX increased the water content of films at 50 and 76% RH, but decreased it at 98% RH. The DP (molar mass) of rAX and rDAX did not affect the moisture uptake of films.

Mechanical properties

Because polysaccharide films are hydrophilic materials, it is important to study the moisture-dependency

Fig. 4 The water sorption isotherms of films from **a** high DP rAXs and **b** low DP rAXs. The results are averages of two measurements
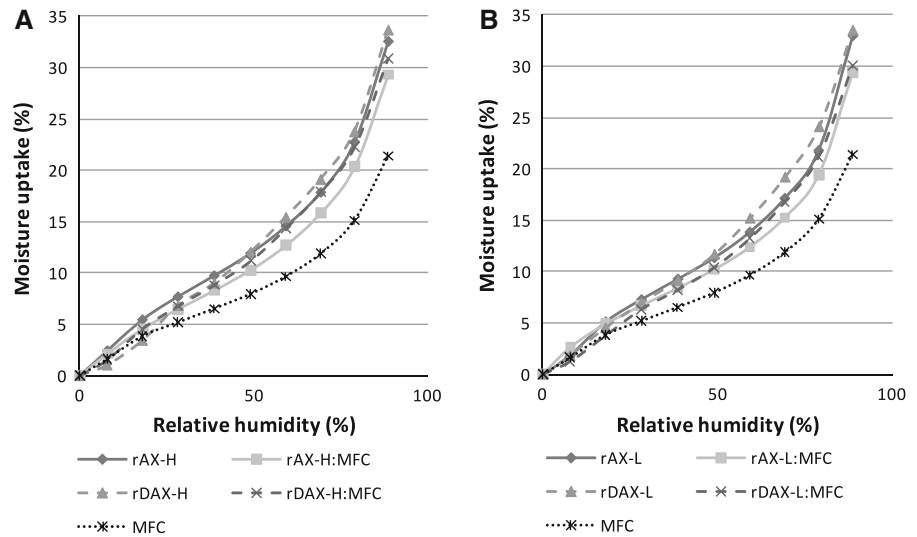
of their mechanical properties. Therefore the storage modulus of films was determined as a function of RH to evaluate the effect of moisture on the stiffness of the films. The results are presented as relative values, i.e., as percentages of the storage modulus of the dry film, to eliminate the effect of variation of specimen dimensions on the results (Fig. 5). As expected, the storage modulus of films decreased with increasing RH, indicating moisture-induced plasticization. Similar behavior was seen earlier for rAX films (Stevanic et al. 2011) and spruce galactoglucomannan films (Mikkonen et al. 2011). The decrease in DS of rAX decreased the softening of films at low RH, but increased it at high RH, regardless of the presence of MFC. Thus, the high crystallinity of rDAX films did not consistently correspond with higher stiffness. As the moisture uptake of rAX and rDAX films at 90% RH was similar despite the fact that rDAX films had crystalline regions that probably absorb only a small amount of water, the amorphous parts of the rDAX films could have swelled more than the totally amorphous films from high DS rAXs, leading to increased softening of the films. As discussed earlier, rDAXs contain structurally diverging populations of arabinoxylans, some of which may be more prone to crystallize. Thus the amorphous part may contain a population of arabinoxylans which swell more at high RH. The relative storage modulus of films was rather similar regardless of the DP of rAX, indicating that the films from rAXs with different chain lengths responded similarly to the low forces applied to the films at the elastic range.
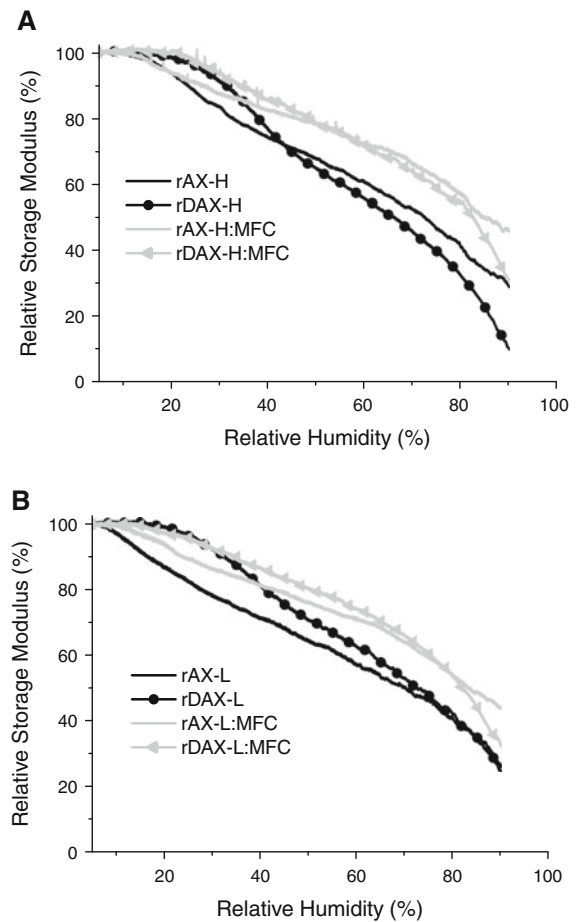

Fig. 5 Relative storage modulus of plain and composite films from **a** high DP rAXs and **b** low DP rAXs as a function of relative humidity

The addition of MFC increased the RH of softening of all films. In general, the relative storage modulus of films containing MFC was higher than that of the plain rAX films at RH values higher than 40%. This indicates reinforcement of films by MFC, but could also be at least partly affected by the decreased moisture content of films at high RH due to the addition of MFC.

The mechanical properties of the films were further evaluated by tensile testing (Fig. 6). Decreasing DS of rAX decreased the tensile strength of films on average by 7.6 MPa and Young's modulus by 426 MPa, but did not affect the elongation at break (Table 6). The effect of DS of rAX on the tensile strength and Young's modulus of the films did not depend on the DP of rAX, as the p-values for the interaction effect were 0.915 and 0.608, respectively (Table 6). Previously, a small decrease in DS of rAX (Ara:Xyl 0.37) increased the tensile strength of films, but films from rAX with Ara:Xyl ratios closer to those of rDAX-H and rDAX-L in the present study (0.30 and 0.20) had lower tensile strength than films from native rAX (Ara:Xyl 0.50) (Höije et al. 2008). Films from debranched guar gum galactomannan studied previously had higher mechanical performance than films from native guar gum galactomannan (Mikkonen et al. 2007). A moderate enzymatic decrease in the DP of guar gum galactomannan, which is originally a much larger polymer than rAX, also increased the tensile strength and elongation at break of films, but a more severe treatment decreased them (Mikkonen et al. 2007). In the present study, a decrease in the DP of rAX decreased the tensile strength of films on average by 33.2 MPa and elongation at break by 7.1%, but Young's modulus was not affected (Table 6). However, the reduction in the tensile strength of rAX films was unexpectedly small, considering that the decrease in the DP of rAX was significant. This could be at least partly explained by the high poly-dispersity of the endoxylanase treated samples, i.e. rAX-L also contained large polymers.

Tensile testing confirmed the reinforcing effect of MFC on rAX (Table 6). The tensile strength of the rAX-H film was 64 ± 6 MPa and that of the rAX-H:MFC film was 95 ± 19 MPa (measurements at 50% RH). The reinforcement by MFC was also high for rDAX-H but, for low DP rAXs, the effect was surprisingly much smaller and not statistically significant (Fig. 6). The addition of MFC combined with a decrease in the DS and DP of rAX greatly increased
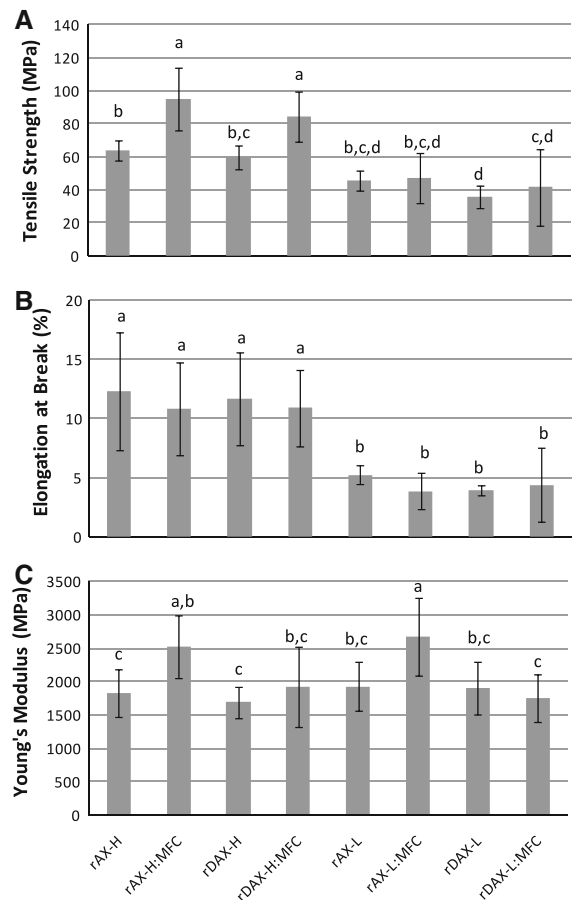

Fig. 6 **a** Tensile strength, **b** elongation at break, and **c** Young's modulus of films. The results are averages from 9–12 measurements, except for rDAX-L:MFC, of which three measurements were done. The *error bars* indicate standard deviations, and the *small letters a, b, c*, and *d* mean statistically significant differences from Tukey's test ($p \leq 0.05$) (the same *letter* on the *bars* means that there is no statistical difference between the values, while *different letters* means that there is a statistical difference)

the brittleness of the films, as only three replicate specimens of rDAX-L:MFC film could be measured with the tensile tester due to fracturing of the film specimens during cutting.

The addition of MFC did not affect the elongation at break of films. In contrast, MFC increased the Young's modulus of films from high DS rAXs, but not that of films from low DS rDAXs ($p = 0.002$) (Table 6). The effect of MFC on the Young's modulus of the films was similar regardless of the DP of rAX, which is in agreement with the results of storage modulus determined with DMA. Thus, according to

Table 6 Estimated values of contrast in the effect of film composition on the tensile strength, elongation at break, and Young's modulus of films

	Tensile strength (MPa)	Elongation at break (%)	Young's modulus (MPa)
DS	−7.6 (0.014[a])	−0.3 (0.671)	−426 (<0.001)
DP	−33.2 (<0.001)	−7.1 (<0.001)	72.3 (0.507)
MFC	15.8 (<0.001)	−0.8 (0.312)	384 (<0.001)
DS/DP	0.3 (0.915)	0.04 (0.963)	55.8 (0.608)
MFC/DS	0.5 (0.870)	−0.6 (0.427)	340 (0.002)
MFC/DP	12.2 (<0.001)	−0.3 (0.667)	82.3 (0.450)
RMSE[b]	12.4	3.2	444

Degrees of freedom for MSError (ANOVA error term) = 75

[a] p value; values below 0.05 indicate statistical significance

[b] RMSE is the square root of MSError and is the average standard deviation between the replicate specimens

tensile testing, the films from high DS rAXs became stiffer with added MFC. This is a property studied in the elastic region of the deformation, while tensile strength is linked to higher deformation at the breaking point of the sample. Low DP of rAX was not a disadvantage in the elastic range studied using low forces but, at higher forces, the shorter xylan chains were not able to stretch and slide across each other as much as the longer chains, resulting in breaking of the film specimens at an earlier stage and at a lower tensile strength. In addition, the hydrogen bonded network of rAX with MFC could have been weaker with lower molar mass of rAX.

The reinforcing effect of MFC on rAX-H and rDAX-H was clearly higher than that of bacterial cellulose on rAX films (Stevanic et al. 2011). The effect of MFC on high DP rAX films was also higher than that on spruce galactoglucomannan films (Mikkonen et al. 2011). Unlike spruce galactoglucomannan, rAX forms cohesive films without an additional plasticizer. A high amount of glycerol as a plasticizer was previously considered to prevent load transfer between matrix and reinforcement (Mikkonen et al. 2010a, b), and decreasing the amount of glycerol increased the reinforcement of spruce galactoglucomannan films by MFC (Mikkonen et al. 2011). However, the reinforcing effect of MFC on spruce galactoglucomannan films was higher than on low DP rAX films, although the molar mass of galactoglucomannan is at the same magnitude or even lower than that of rAX-L in the present study (Willför et al. 2008). The diminished reinforcement effect of MFC on films from low DP rAXs may be a result of impaired interactions of MFC with rAX-L and rDAX-L. The

action of endoxylanases is generally restricted by L-arabinofuranosyl side groups, and thus enzymatic hydrolysis is expected to first proceed on the least substituted regions of the xylan backbone. The same regions of the xylan chain may be those responsible for tight hydrogen bonds with MFC, as a decrease in the Ara:Xyl ratio and an increasing number of unsubstituted xylopyranosyl units increases the amount of adsorbed arabinoxylan on cellulose (Köhnke et al. 2011). Indeed, enzymatic hydrolysis of wheat arabinoxylan from 336,000 to 129,000 g/mol significantly reduced its adsorption on the nanocellulose surface, as revealed by the quartz crystal microbalance measurements (Eronen et al. 2011). However, hydrolysis of less substituted regions of the xylan backbone does not explain the low reinforcement of rDAX-L films, as new unsubstituted xylopyranosyl residues were created by debranching with α-arabinofuranosidase.

Conclusions

Controlled enzymatic modification was performed on rAX by decreasing its DS and DP to prepare a set of samples to mimic the diversity of naturally occurring arabinoxylans. Films were successfully prepared from native and modified rAX samples with and without the addition of MFC. The addition of MFC and the chemical structure of rAX affected the properties of the films, and the reinforcing effect of MFC clearly depended on the structure of rAX. Polarizing fibers were visualized by microscopy in films containing MFC and, in addition, polarizing structures formed in the composite films from low DS rDAXs, indicating

interactions between MFC and debranched rDAX. This was also seen as an increased haze in MFC-reinforced films from low DS rDAXs. However, although the crystallinity of rAX in the films was increased by the enzymatic modifications, it was not significantly affected by MFC. The addition of MFC somewhat decreased the moisture uptake of films and clearly increased the RH of softening of the films. Surprisingly, MFC greatly increased the tensile strength of films from high molar mass rAXs, but not that of films from low molar mass rAXs. This is the first study combining MFC with structurally different arabinoxylans, and the results indicate that using MFC as reinforcement of films from low DS and DP arabinoxylans, such as the potential forest biorefinery products from softwoods, may be challenging. However, the low DP and DS sample studied in the present work does not fully mimic softwood arabinoxylans, which in addition to the neutral α-L-arabinofuranosyl side groups also carry acidic 4-O-methylglucopyranosyl uronic acid substituents.

References

ASTM (2007) Standard test method for haze and light transmittance of transparent plastics, method ASTM D 1003–07

Bengtsson S, Åman P, Andersson RE (1992) Structural studies on water-soluble arabinoxylans in rye grain using enzymatic hydrolysis. Carbohydr Polym 17:277–284

Ebringerová A, Heinze T (2000) Naturally occuring xylans structures, isolation procedures and properties. Macromol Rapid Commun 21:542–556

Eronen P, Heikkinen S, Österberg M, Tenkanen M, Laine J (2011) Interactions of structurally different hemicelluloses with nanofibrillar cellulose. Carbohydr Polym 86:1281–1290

Gatenholm P, Bodin A, Gröndahl M, Dammström S, Eriksson L (2008) Polymeric film or coating comprising hemicellulose. Patent US 7427643 B2, Sep 23, 2008

Gröndahl M, Eriksson L, Gatenholm P (2004) Material properties of plasticized hardwood xylans for potential application as oxygen barrier films. Biomacromolecules 5:1528–1535

Gröndahl M, Eriksson L, Gatenholm P, Hjertberg T (2008) Polymeric film or coating comprising hemicellulose. Patent Application WO2008103123 A2, Aug 28, 2008

Guilbert S, Gontard N, Gorris LGM (1996) Prolongation of the shelf-life of perishable food products using biodegradable films and coatings. LWT Food Sci Technol 29:10–17

Guinier A (1994) X-ray diffraction in crystals, imperfect crystals, and amorphous bodies. Dover Publications Inc., New York

Hettrich K, Fischer S, Schröder N, Engelhardt J, Drechsler U, Loth F (2006) Derivatization and characterization of xylan from oat spelts. Macromol Symp 232:37–48

Höije A, Sternemalm E, Heikkinen S, Tenkanen M, Gatenholm P (2008) Material properties of films from enzymatically tailored arabinoxylans. Biomacromolecules 9:2042–2047

Izydorczyk MS, Biliaderis CG (1995) Cereal arabinoxylans: advances in structure and physicochemical properties. Carbohydr Polym 28:33–48

Köhnke T, Pujolras C, Roubroeks JP, Gatenholm P (2008) The effect of barley husk arabinoxylan adsorption on the properties of cellulose fibres. Cellulose 15:537–546

Köhnke T, Östlund Å, Brelid H (2011) Adsorption of arabinoxylan on cellulosic surfaces: influence of degree of substitution and substitution pattern on adsorption characteristics. Biomacromolecules 12:2633–2641

Mikkonen KS, Rita H, Helén H, Talja RA, Hyvönen L, Tenkanen M (2007) Effect of polysaccharide structure on mechanical and thermal properties of galactomannan-based films. Biomacromolecules 8:3198–3205

Mikkonen KS, Heikkinen S, Soovre A, Peura M, Serimaa R, Talja RA, Helén H, Hyvönen L, Tenkanen M (2009) Films from oat spelt arabinoxylan plasticized with glycerol and sorbitol. J Appl Polym Sci 114:457–466

Mikkonen KS, Heikkilä MI, Helén H, Hyvönen L, Tenkanen M (2010a) Spruce galactoglucomannan films show promising barrier properties. Carbohydr Polym 79:1107–1112

Mikkonen KS, Mathew AP, Pirkkalainen K, Serimaa R, Xu C, Willför S, Oksman K, Tenkanen M (2010b) Glucomannan composite films with cellulose nanowhiskers. Cellulose 17:69–81

Mikkonen KS, Stevanic JS, Joly C, Dole P, Pirkkalainen K, Serimaa R, Salmén L, Tenkanen M (2011) Composite films from spruce galactoglucomannans with microfibrillated spruce wood cellulose. Cellulose 18:713–726

Nieduszynski IA, Marchessault RH (1972) Structure of β, D(1 $\rightarrow$ 4')-xylan hydrate. Biopolymers 11:1335–1344

Nisperos-Carriedo M (1994) Edible coatings and films based on polysaccharides. In: Baldwin EA, Nisperos-Carriedo M, Krochta JM (eds) Edible coatings and films to improve food quality. Technomic Publishing Company, Lancaster, pp 305–335

Pääkkö M, Ankerfors M, Kosonen H, Nykänen A, Ahola M, Österberg M, Ruokolainen J, Laine J, Larsson PT, Ikkala O, Lindström T (2007) Enzymatic hydrolysis combined with mechanical shearing and high-pressure homogenization for nanoscale cellulose fibrils and strong gels. Biomacromolecules 8:1934–1941

Peng X, Ren J, Zhong L, Sun R (2011) Nanocomposite films based on xylan-rich hemicelluloses and cellulose nanofibers with enhanced mechanical properties. Biomacromolecules 12:3321–3329

Pitkänen L, Virkki L, Tenkanen M, Tuomainen P (2009) Comprehensive multidetector HPSEC study on solution properties of cereal arabinoxylans in aqueous and DMSO solutions. Biomacromolecules 10:1962–1969

Ramírez F, Puls J, Zúñiga V, Saake B (2008) Sorption of corn cob and oat spelt arabinoxylan onto softwood kraft pulp. Holzforschung 62:329–337

Saxena A, Elder TJ, Pan S, Ragauskas AJ (2009) Novel nano-cellulosic xylan composite film. Composites Part B 40: 727–730

Sehaqui H, Liu A, Zhou Q, Berglund L (2010) Fast preparation procedure for large, flat cellulose and cellulose/inorganic nanopaper structures. Biomacromolecules 11:2195–2198

Shen L, Patel MK (2008) Life cycle assessment of polysaccharide materials: a review. J Polym Environ 16:154–167

Sjöström E (1993) Wood chemistry fundamentals and applications. Academic Press, Inc., San Diego

Sternemalm E, Höije A, Gatenholm P (2008) Effect of arabinose substitution on the material properties of arabinoxylan films. Carbohydr Res 343:753–757

Stevanic JS, Joly C, Mikkonen KS, Pirkkalainen K, Serimaa R, Rémond C, Toriz G, Gatenholm P, Tenkanen M, Salmén L (2011) Bacterial nanocellulose-reinforced arabinoxylan films. J Appl Polym Sci 122:1030–1039

Sun RC, Tomkinson J, Wang YX, Xiao B (2000) Physico-chemical and structural characterization of hemicelluloses from wheat straw by alkaline peroxide extraction. Polymer 41:2647–2656

Sundberg A, Sundberg K, Lillandt C, Holmbom B (1996) Determination of hemicelluloses and pectins in wood and pulp fibres by acid methanolysis and gas chromatography. Nord Pulp Pap Res J 11(216–219):226

Wågberg L, Decher G, Norgren M, Lindström T, Ankerfors M, Axnäs K (2008) The build-up of polyelectrolyte multilayers of microfibrillated cellulose and cationic polyelectrolytes. Langmuir 24:784–795

Willför S, Sundberg K, Tenkanen M, Holmbom B (2008) Spruce-derived mannans: a potential raw material for hydrocolloids and novel advanced natural materials. Carbohydr Polym 72:197–210

Zhang Y, Pitkänen L, Douglade J, Tenkanen M, Remond C, Joly C (2011) Wheat bran arabinoxylans: chemical structure and film properties of three isolated fractions. Carbohydr Polym 86:1230–1235